JOURNAL OF MATERIALS SCIENCE 31 (1996) 4261–4265

The effect of the microstructure, phase and chemical composition on the humidity sensing characteristics of SnO_2–Fe_2O_3 spray deposited thin films using different iron salts

I. STAMBOLOVA, K. KONSTANTINOV
Bulgarian Academy of Sciences, Institute of General & Inorganic Chemistry, Acad. G. Bonchev Blvd., Bl. 11, 1113 Sofia, Bulgaria

This paper describes the correlation between the nature of iron salt in the spray solution and the microstructure, phase and chemical composition of SnO_2–Fe_2O_3 thin films, deposited by spray technique. The dependence between humidity sensitive parameters and the chemical and microstructural characteristics have also been studied.

It was found that the films exhibit an homogeneous fine grain structure. Part of the introduced iron precipitates in large crystallites on the surface. The fine grain film structure has been obtained using both $Fe_2(C_2O_4)_3$ or $Fe(NH)_4(SO_4)_2 \cdot 12H_2O$ as iron precursors. When iron oxalate is used, finer microstructure is obtained (10–20 nm smaller grain sizes). The concentration of doping element in the homogeneous layer is independent of the type of the used iron salt. In the large crystallites, however, when an organic precursor is used the iron content is twice as low than in the case of the iron sulphate. The quantity and type of iron salt used strongly affect the humidity, sensitivity and electrical resistance of the layers.

1. Introduction

Many industrial processes, human health, solid state electronic equipment and optimal functioning of various home appliances are affected by extreme relative humidity and consequently necessitates humidity sensing and control. Recently, various metal oxides such as $MgAl_2O_4$ [1], $MgCr_2O_4$–TiO_2 [2], Fe_2O_3 [3, 4] and MnO_2 [5] have been investigated as humidity sensitive materials.

In spite of the advantages of SnO_2, the report concerning humidity sensors based on pure and doped SnO_2 are quite rare [6]. In a previous paper we have proposed the use of sprayed SnO_2–Fe_2O_3 thin films as humidity sensors with good sensitivity, response and recovery times [7].

The aim of the present paper is to obtain detailed information and better understanding of the influence of the iron precursor, used for the preparation of films on their microstructure, phase and chemical composition. Also, the correlation between the investigated film characteristics and their humidity sensitive properties has been studied.

2. Experimental procedure

The films were obtained by spraying solutions, containing certain quantities of 0.2 M $SnCl_4$ in ethanol and 0.2 M solutions of two different iron salts ($Fe(NH)_4(SO_4)_2 \cdot 12H_2O$, salt A; $Fe_2(C_2O_4)_3$, salt B) in ethanol + water.

In Table I the molar Fe:Sn ratios in the solutions and their code names are shown. The solutions were sprayed onto hollow quartz cylinders (length 10 mm, diameter 6 mm) with a flow rate of 0.04 $cm^3 s^{-1}$. Before the deposition the substrates were cleaned by standard procedures and were tempered at 480 °C for 10 min. The films were thermally treated in oxygen atmosphere at 900 °C for 30 min. The thickness of the films obtained was about 250 nm. Sensor elements were prepared following the design described in [8].

The sensors were mounted in test chambers which were closed flasks partially filled with saturated salt solutions in order to obtain certain relative humidity (*RH*). The humidity sensitivity, response and recovery times were estimated by the electrical resistance (*R*) change. The electrical resistance was measured with a conventional multimeter. The relationships $R = f(RH)$ were measured by sealing the sensor element in the flask with a definite humidity. *R* of the sensor in dry air was measured in the same way using a flask with a dryer. The response and recovery times were evaluated by the electrical resistance change on increasing the humidity from 0–93% and on decreasing it from 93–0%, respectively.

The phase composition and lattice parameters of the films were studied by X-ray diffraction (XRD), using CoK_α radiation. The morphology and chemical composition were investigated by scanning electron microscopy (SEM) and energy dispersive X-ray (EDX) analysis.

0022–2461

TABLE I Fe:Sn molar ratios in the spray solutions and their corresponding code names in dependence of the used iron salt

Fe:Sn molar ratios in the spray solution	Solution code name	
	Used salt $Fe(NH)_4(SO_4)_2 \cdot 12H_2O$ (salt A)	Used salt $Fe_2(C_2O_4)_3$ (Salt B)
1:1	1A	1B
1:4	2A	2B
1:6	3A	3B
1:9	4A	4B
1:19	5A	5B

3. Results and discussion

The analysis of the experimental results show that both electrical resistance and humidity sensitivity are strongly influenced by the quantity of the dopant and nature of iron salt, introduced into the spray solution. The films obtained from $SnCl_4$ and $Fe_2(C_2O_4)_3$ possess very high electrical resistance at 20 °C in dry air ($R > 10^9$ Ohm). Due to this fact some of the $\log R = f(RH)$ curves have been extrapolated above this value. As Fig. 1 shows, the layers deposited from solutions 1A–5A have a steplike region in the curve $\log R = f(RH)$. When the iron content increases this region nearly disappears. The layers obtained from solutions 1B–5B show smoother characteristics, exhibiting a slight step at 65–85% *RH*. The response times of the 2B–5B films are shorter than the corresponding 2A–5A films. This parameter is almost the same for 1A and 1B films. The recovery times of 1B–4B layers are shorter than the respective of 1A–4A layers. The recovery times of 5A and 5B films are similar. These relationships are shown in Fig. 2 and Fig. 3.

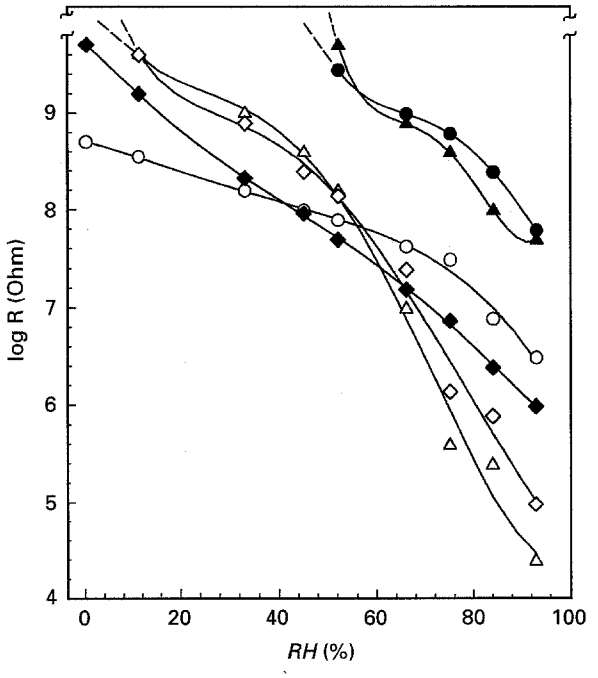

Figure 1 Dependence of resistance versus relative humidity at 20 °C of SnO_2–Fe_2O_3 thin films. Fe:Sn = 1:1 (solution 1A) ○; Fe:Sn = 1:1 (solution 1B) ●; Fe:Sn = 1:4 (solution 2A) △; Fe:Sn = 1:4 (solution 2B) ▲; Fe:Sn = 1:19 (solution 5A) ◇; Fe:Sn = 1:19 (solution 5B) ◆.

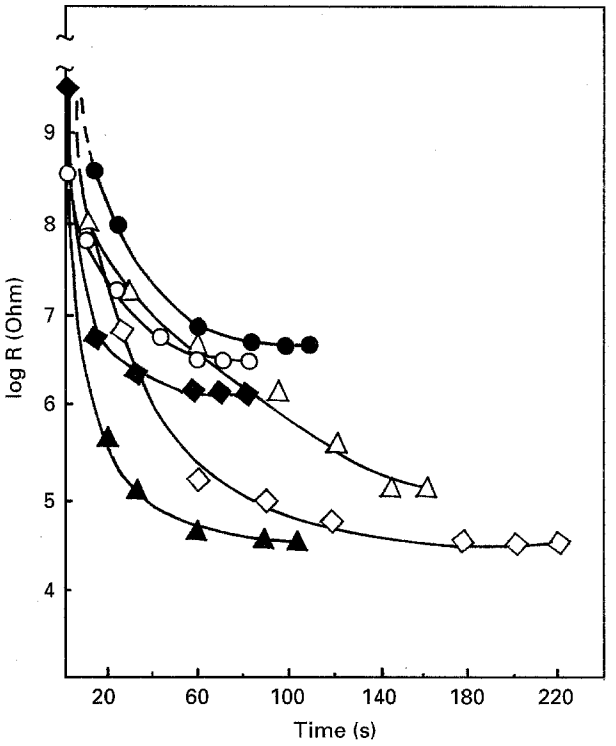

Figure 2 Humidity response time at 20 °C when *RH* changes from 0 to 93%. Fe:Sn = 1:1 (solution 1A) ○; Fe:Sn = 1:1 (solution 1B) ●; Fe:Sn = 1:4 (solution 2A) △; Fe:Sn = 1:4 (solution 2B) ▲; Fe:Sn = 1:19 (solution 5A) ◇; Fe:Sn = 1:19 (solution 5B) ◆.

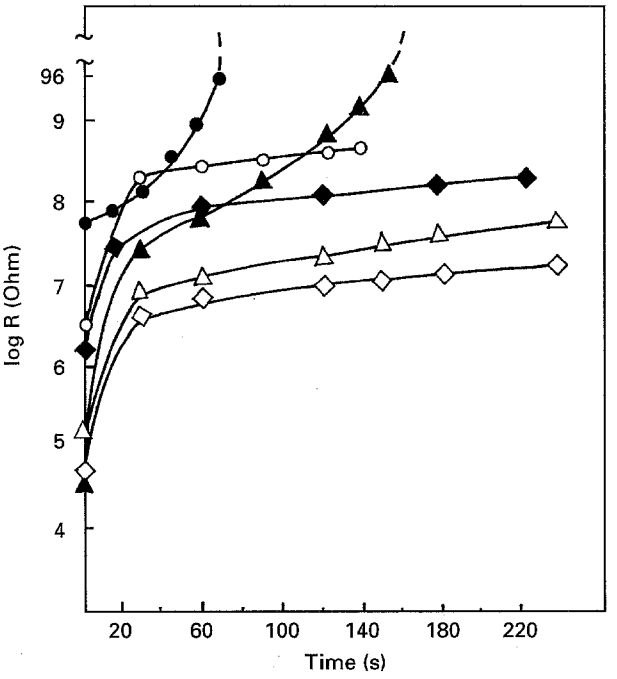

Figure 3 Humidity recovery time at 20 °C when *RH* changes from 93 to 0%. Fe:Sn = 1:1 (solution 1A) ○; Fe:Sn = 1:1 (solution 1B) ●; Fe:Sn = 1:4 (solution 2A) △; Fe:Sn = 1:4 (solution 2B) ▲; Fe:Sn = 1:19 (solution 5A) ◇; Fe:Sn = 1:19 (solution 5B) ◆.

The XRD results concerning the phase composition and lattice parameters of SnO_2 are very similar for both 1A–5A and 1B–5B films. The XRD analysis of films obtained from solutions with ratios Fe:Sn = 1:19, 1:9 and 1:6 shows that they are monophase (α-SnO_2 cassiterite). For higher Fe:Sn ratios (films 1A, 2A, 1B and 2B) the analysis indicates

the presence of two phases – cassiterite and α-Fe_2O_3 haematite (Fig. 4(a, b)). In the films obtained from organic precursor, however, the quantity of haematite is about two times lower than in the films obtained from $Fe(NH)_4(SO_4)_2 \cdot 12H_2O$.

Table II presents the variation of the lattice parameters of SnO_2–Fe_2O_3 films. The increasing of Fe:Sn ratio in the solution results in a lower value of the *c* parameter and in slightly higher values for *a* and *b*. Therefore, the iron cations are incorporated into the SnO_2 crystal lattice and create a solid solution.

The SEM observations of the microstructure reveal that all layers possess a fine grain size microstructure and few large crystallites located on the surface (Fig. 5). The 1B–5B films have finer microstructure (about 20 nm smaller grain size for the same Fe:Sn ratios) than the 1A–5A films (Table III, Fig. 6). The layer 1B has the finest microstructure. The increase of the iron concentration in the solution results in the decreasing of the grain sizes (Table III).

Tables IV and V present the EDX results for both 1A–5A and 1B–5B films. The iron content in the layers is much lower than the initial quantity in the solution. We found that the chemical composition of both the basic layer and the large crystallites are influenced by the nature of used iron salt. When salt A is used the Fe predominantly accumulates in the large crystallites and this tendency is more pronounced when the Fe:Sn ratio in the solution increases. The Fe content for films obtained from organic precursor (salt B) is almost similar in both the large crystallites and the basic layer. Contrary to the above, this rule is not in agreement for the 1B film (where the iron content in the large crystallites is about three times higher than in the basic layer).

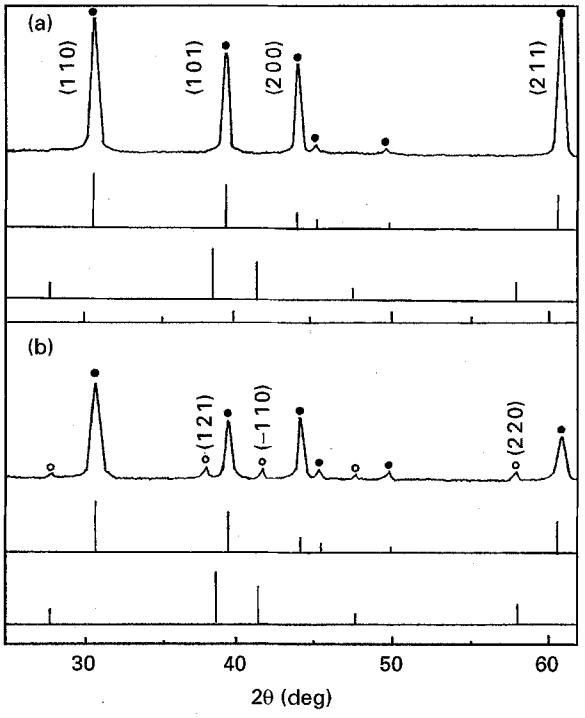

Figure 4 Typical XRD patterns for SnO_2–Fe_2O_3 thin films obtained from solutions with ratios Fe:Sn 1:6 (a) and 1:1 (b). The ASTM patterns of α-SnO_2 (cassiterite) and Fe_2O_3 (haematite) are also given for reference. ● SnO_2; ○ Fe_2O_3.

TABLE II Dependence of the lattice parameters versus Fe:Sn molar ratio in the spray solution

Fe:Sn molar ratio in the spray solution	α-SnO_2 lattice parameters in SnO_2–Fe_2O_3 thin films	
	$a = b$ (nm)	c (nm)
1:1	0.4695 (2)	0.3162 (1)
1:4	0.4695 (1)	0.3167 (1)
1:6	0.4698 (3)	0.3168 (3)
1:9	0.4687 (2)	0.3178 (2)
1:19	0.4687 (2)	0.3176 (2)

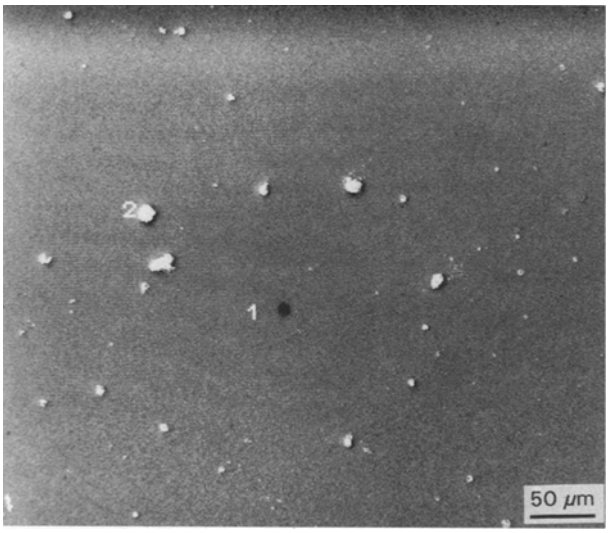

Figure 5 Typical SEM photograph of SnO_2–Fe_2O_3 thin film. Region 1 presents the homogeneous film microstructure and Region 2 shows the large crystallite on the surface.

TABLE III Effect of iron concentration on the grain size crystallites of SnO_2–Fe_2O_3 thin films, using different iron precursors

Fe:Sn molar ratio in the spray solution	Grain size (nm)	
	$Fe(NH)_4(SO_4)_2 \cdot 12H_2O$	$Fe_2(C_2O_4)_3$
1:1	52	40
1:4	60	50
1:6	75	55
1:9	95	75
1:19	160	140

Comparison of the data in Tables IV and V reveals that the iron content in the basic film is not influenced by the type of the iron salt used. This explains the similar changes in the lattice parameters of SnO_2 for the films obtained from salt A and salt B. In addition, the higher Fe content in the large crystallites of 1A–5A films explains the stronger presence of the secondary haematite phase.

On the basis of the above results it is possible to explain the humidity sensitive properties of the films. It may be expected that in the chemical reactions

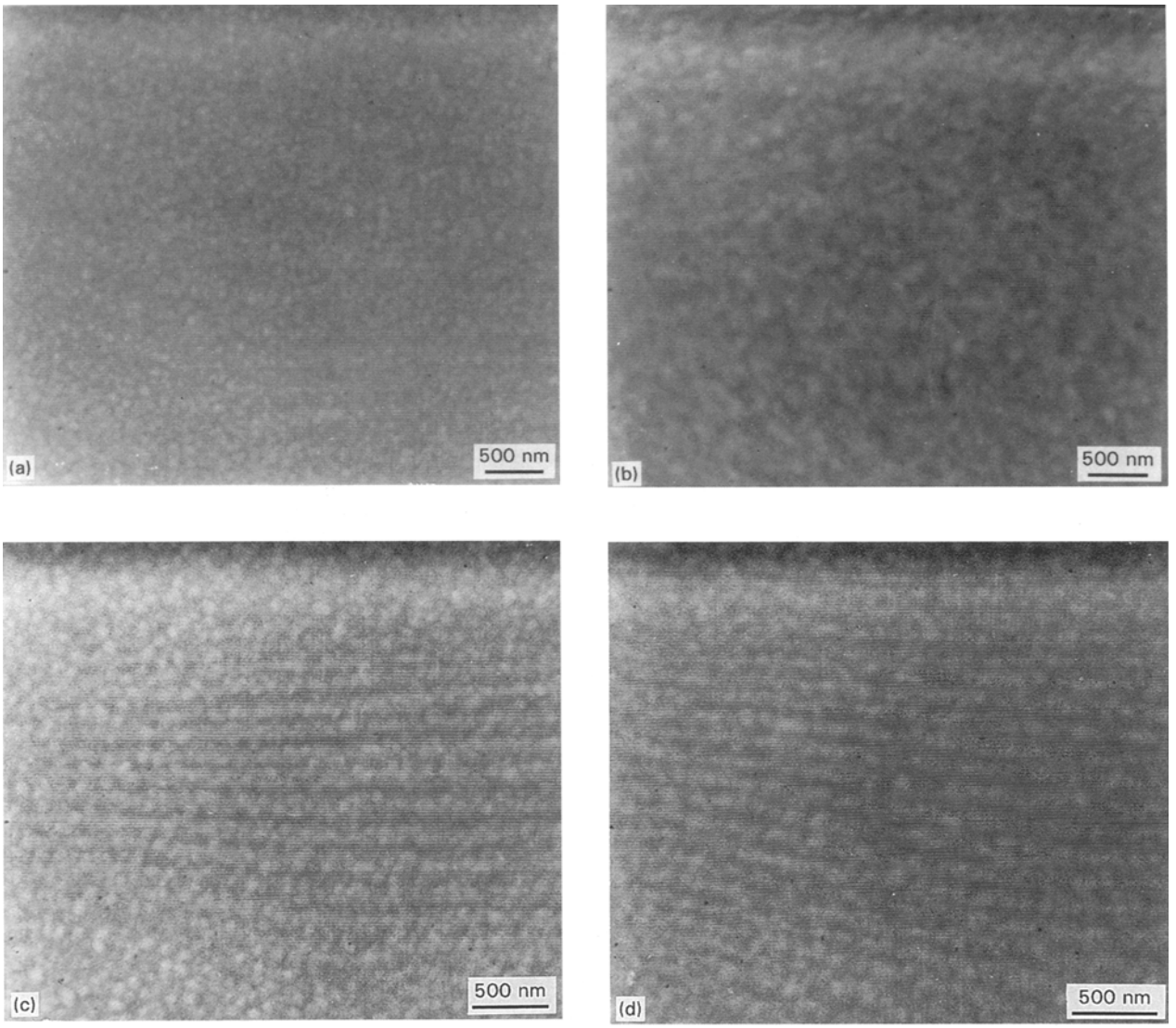

Figure 6 SEM photographs of SnO_2–Fe_2O_3 thin films obtained from solutions 2A (a), 3A (b), 3B (c) and 4B (d).

TABLE IV EDX results for SnO_2–Fe_2O_3 thin films, using $Fe(NH)_4(SO_4)_2 \cdot 12H_2O$ as iron precursor

Fe:Sn molar ratio in the spray system	Fe:Sn ratio in the film	Fe:Sn ratio in the large crystallites
1:1	0.13	0.76
1:4	0.08	0.24
1:6	0.06	0.16
1:9	0.05	0.10
1:19	0.03	0.05

TABLE V EDX results for SnO_2–Fe_2O_3 thin films, using $Fe_2(C_2O_4)_3$ as iron precursor

Fe:Sn molar ratio in the spray solution	Fe:Sn ratio in the film	Fe:Sn ratio in the large crystallites
1:1	0.11	0.38
1:4	0.08	0.11
1:6	0.06	0.07
1:9	0.03	0.04
1:19	0.02	0.03

taking part on the surface, atoms from both the basic layer and large crystallites are involved. As the above mentioned results show, the 3B–5B films are characterised with relatively small difference in the chemical composition between the basic layer and the large crystallites. Therefore, similar types and kinetics of chemical reactions can be expected there. This will lead to linear change of $R = f(RH)$ (see the dependence for film 5B in Fig. 1). For films 1B and 2B, however, the higher iron content in the large crystallites (in comparison to the basic layer) determines a steplike region in the $R = f(RH)$ curve. The same reasoning can be applied to explain the humidity sensitive properties of the films obtained from $SnCl_4$ and inorganic iron salt. Finally, the shorter recovery times of 1B–4B films compared to the corresponding times of 1A–4A films are due to the finer microstructure ensuring more sites for H_2O adsorption/desorption processes.

4. Conclusions

The effect of the type of the iron salt in the spray solution on the microstructure, phase and chemical

composition of the humidity sensitive SnO_2–Fe_2O_3 thin films have been investigated. It was established that a small quantity of the iron is incorporated into the SnO_2 lattice. This causes a decrease of the *c* parameter and an increase of the *a* and *b* parameters. The films obtained from $SnCl_4 + Fe_2(C_2O_4)_3$ possess a finer microstructure than the films obtained from $SnCl_4 + Fe(NH)_4(SO_4)_2 \cdot 12H_2O$. The iron precipitates predominantly in the large crystallites on the surface when $Fe(NH)_4(SO_4)_2 \cdot 12H_2O$ is used. In the case of $Fe_2(C_2O_4)_3$ the distribution of iron in the film is more homogeneous. Therefore, the use of organic iron precursor is more favourable. The different structural and chemical characteristics of the layers obtained from different iron salts affect the humidity sensitive parameters. The use of $Fe_2(C_2O_4)_3$ generally leads to smoother $\log R(RH)$ dependencies without strong steplike regions and shorter response time. When $Fe(HN)_4(SO_4)_2 \cdot 12H_2O$ is used, the humidity sensitive characteristics of the layers exhibit more complex behaviour.

References

1. G. GUSMANO, G. MONTESPERELLI, E. TRAVERSA and A. BEARZOTTI, *Sens. Act. B* **13–14** (1993) 525.
2. T. Y. KIM, D. H. LEE, Y. C. SHIM, J. U. BU and S. T. KIM, *Ibid.* **9** (1992) 221.
3. C. CANTALINI and M. PELINO, *J. Amer. Ceram. Soc.* **75** (1992) 546.
4. M. FUKAZAMI, H. MATUZAKI and K. HARA, *Sens. Act. B* **13–14** (1993) 521.
5. C.-N. XU and K. MIYAZAKI, *Ibid.* **13–14** (1993) 523.
6. G. HUYBERECHTS, M. HONORE and J. ROGGEN, *Ibid.* **13–14** (1993) 281.
7. T. RATCHEVA, I. STAMBOLOVA and T. DONCHEV, *J. Mater. Sci.* **29** (1994) 281.
8. T. RATCHEVA, I. STAMBOLOVA and K. KONSTANTINOV, *Thin Solid Films* **217** (1992) 187.

Received 8 August
and accepted 21 December 1995